

The QCD Phase Diagram at Nonzero Temperature, Baryon and Isospin Chemical Potentials in Random Matrix Theory

B. Klein,¹ D. Toublan,² and J.J.M. Verbaarschot¹

¹*Department of Physics and Astronomy, State University of New York at Stony Brook, Stony Brook, NY 11794-3800*

²*Department of Physics, University of Illinois at Urbana-Champaign, Urbana, IL 61801-3080*

(Dated: June 16, 2018)

We introduce a random matrix model with the symmetries of QCD at finite temperature and chemical potentials for baryon number and isospin. We analyze the phase diagram of this model in the chemical potential plane for different temperatures and quark masses. We find a rich phase structure with five different phases separated by both first and second order lines. The phases are characterized by the pion condensate and the chiral condensate for *each* of the flavors. In agreement with lattice simulations, we find that in the phase with zero pion condensate the critical temperature depends in the same way on the baryon number chemical potential and on the isospin chemical potential. At nonzero quark mass, we remarkably find that the critical end point at nonzero temperature and baryon chemical potential is split in two by an arbitrarily small isospin chemical potential. As a consequence, there are *two* crossovers that separate the hadronic phase from the quark-gluon plasma phase at high temperature. Detailed analytical results are obtained at zero temperature and in the chiral limit.

I. INTRODUCTION

Currently, there is a strong interest in exploring the phase diagram of QCD at finite baryon density. A large number of possible phases have been suggested for QCD at finite baryon density (see [1, 2] for a review). However, at this moment, the existence of any of these phases has been confirmed neither by first principle calculations nor by the phenomenology of heavy ion collisions and neutron stars. Because of the phase of the fermion determinant, standard Monte-Carlo simulations are only possible for small values of the chemical potential [3, 4, 5, 6, 7, 8, 9]. Neutron stars are probably the most likely candidates for high baryon density physics, but they are hard to observe and only few parameters can be measured accurately. Relativistic heavy ion collisions explore the region of low baryon density and high temperature but give a complex picture of QCD at finite density. However, an experimental observation of a tricritical point might be within the realm of possibilities. Such a tricritical point was predicted on the basis of effective potentials [10] and simplified models such as random matrix models [11] and Nambu-type models [12]. Furthermore, in both neutron stars and relativistic heavy ion collisions, the isospin density is different from zero. It is therefore important both phenomenologically and theoretically to study the influence of isospin on the phase diagram of QCD at nonzero baryon chemical potential.

Our main goal is to study the phase diagram of QCD at nonzero temperature and chemical potentials for baryon number and for isospin. The phase diagram of QCD with any of these external parameters equal to zero has already been studied in a variety of ways. In particular, because lattice simulations are possible at nonzero isospin chemical potential [13, 14], the plane of zero baryon chemical potential has been understood best. At zero temperature, we expect a sec-

ond order phase transition to a phase of condensed pions at an isospin chemical potential equal to half the pion mass. Such type of transition occurs in any QCD-like theory with a chemical potential for the charge of a Goldstone boson [15, 16, 17, 18, 19, 20, 21, 22, 23] [24, 25, 26]. This prediction from effective Lagrangians has been confirmed by numerous lattice QCD simulations [14, 27, 28, 29, 30, 31, 32, 33, 34]. From lattice simulations [14, 34] and a one-loop analysis of the effective Lagrangian [23, 25] it also follows that the second order line changes into a first order line at a tricritical point with critical chemical potential and temperature on the scale of the pion mass. At nonzero baryon chemical potential, analytical results have been obtained for asymptotically large values of the chemical potential where QCD can be analyzed perturbatively [35, 36]. Lattice QCD simulations are only reliable for small values of the chemical potential [3, 4, 6]. This leaves us with the bulk of the μ_B - T -plane which could only be analyzed in simplified models such as Nambu Jona-Lasinio models [12, 37], instanton liquid models [38] and random matrix models [11].

Random matrix models were introduced in the context of QCD to describe the correlations of the low-lying eigenvalues of the QCD Dirac operator [39, 40]. It was shown that these models are equivalent to the mass term of a suitably chosen chiral Lagrangian which is determined uniquely by the symmetries of the underlying microscopic theory [41, 42, 43, 44]. Therefore, in the chiral limit, chiral Random Matrix Theories provide an exact analytical description of the low-lying Dirac spectrum.

In this article we use a Random Matrix Theory as a schematic model for phase transitions in QCD at nonzero temperature and chemical potentials. Such a model was first introduced in [45] to describe the chiral phase transition in QCD at nonzero temperature. Even more successful was the application of Random Matrix Theory to QCD at nonzero baryon chemical potential. First, the

failure of the quenched approximation was explained analytically [46]. Second, a tricritical point was found in a model at nonzero baryon chemical potential and temperature [11]. Third, algorithms for QCD at finite density could be investigated in detail [47, 48]. Fourth, the static part of effective Lagrangians for QCD with a chemical potential for the charge of Goldstone bosons can be derived from a chiral random matrix model [17]. In spite of the schematic nature of the random matrix model, we hope that it will teach us more about the plethora of possible phases that may occur in QCD.

The organization of this paper is as follows. In section II, we deduce from general arguments the expected features of the QCD phase diagram for nonzero temperature, baryon and isospin chemical potentials. In section III, we introduce our random matrix model. In section IV, we derive an effective partition function in terms of the meson fields and reproduce the mean field results obtained from a chiral Lagrangian. The phase diagram resulting from the random matrix model is obtained in section V. Concluding remarks are made in section VI.

II. QCD AT NONZERO CHEMICAL POTENTIALS AND TEMPERATURE

The QCD partition function at nonzero temperature and a chemical potential for each quark flavor is given by

$$\left\langle \prod_{f=1}^{N_f} \det(D + m_f + \mu_f \gamma_0) \right\rangle \quad (2.1)$$

where the Euclidean Dirac operator is given by $D = \gamma_\mu(\partial_\mu + iA_\mu)$ with γ_μ the Euclidean γ -matrices, and A_μ is an $SU(N_c)$ valued gauge potential. The quark masses are denoted by m_f , and μ_f is the chemical potential for each flavor. The average is over the Euclidean Yang-Mills action. Below we mainly focus on QCD with two flavors and nonzero baryon number and isospin chemical potential. In that case, the baryon number and isospin chemical potential are defined by

$$\mu_B = \frac{1}{2}(\mu_1 + \mu_2), \quad (2.2)$$

$$\mu_I = \frac{1}{2}(\mu_1 - \mu_2). \quad (2.3)$$

Before discussing the possible phases of random matrix models with the symmetries of the QCD partition function, we first make some general remarks on its phase diagram at nonzero temperature, isospin and baryon chemical potentials.

The case of $\mu_B = 0$ and m_π , $T \ll \Lambda_{\text{QCD}}$ can be described in terms of a chiral Lagrangian. This Lagrangian has been analyzed to one-loop order [23, 25]. At low T , a second order phase transition to a pion condensation phase was found at $\mu_I = m_\pi/2$ where m_π is the physical pion mass. For $\mu_I > m_\pi/2$ the chiral condensates rotate

into a pion condensate, denoted by ρ , and approach zero for $\mu_I \gg m_\pi/2$. Since a baryon chemical potential only excites states for μ_B larger than the nucleon mass, we expect this second order line to persist in the μ_I - μ_B -plane and to be parallel to the μ_B axis.

The $\mu_I = 0$ plane was discussed in detail in [11]. We expect a region with broken chiral symmetry (with chiral condensates $\langle \bar{u}u \rangle$ and $\langle \bar{d}d \rangle$ both nonzero) separated from the region of unbroken chiral symmetry by a first order curve, denoted by $\mu_c(T)$, from the tricritical point to the $T = 0$ axis and a second order curve from the tricritical point to the $\mu_B = 0$ axis.

For μ_I and μ_B both nonzero, there are eight possible phases with either of the chiral condensates, $\langle \bar{u}u \rangle$, or $\langle \bar{d}d \rangle$, or the pion condensate $\rho = \frac{1}{2}(\langle \bar{u}\gamma_5 d \rangle - \langle \bar{d}\gamma_5 u \rangle)$ equal to zero or not. Since the chemical potentials for the two flavors are different, there is no reason to expect that $\langle \bar{u}u \rangle = \langle \bar{d}d \rangle$.

In the limit $\mu_1 \gg \Lambda_{\text{QCD}}$, one flavor decouples and we are in a situation with only one flavor at nonzero chemical potential. In this case, we expect that $\langle \bar{u}u \rangle = 0$ and $\langle \bar{d}d \rangle \neq 0$ for $\mu_2 < \mu_c(T)$ but vanishes across the first order transition curve for $\mu_2 > \mu_c(T)$.

For $\mu_B = 0$, we have that $\mu_2 = -\mu_1$. Using that

$$\det(D + m - \mu_1 \gamma_0) = \det^*(D + m + \mu_1 \gamma_0), \quad (2.4)$$

we find that for equal quark masses the partition function (2.1) is the phase quenched partition function for two flavors [13, 18].

III. RANDOM MATRIX MODEL

In this article we study a random matrix model for QCD at nonzero chemical potentials and temperature. The idea is to replace the matrix elements of the Dirac operator by Gaussian random variables subject only to the global symmetries of the QCD partition function. The dependence on the temperature and chemical potentials enters through external fields structured according to these symmetries.

Our guiding principle for constructing a random matrix model is dictated by the global symmetries of the QCD partition function. At zero temperature and chemical potential, this amounts to replacing the matrix elements of the Dirac operator by Gaussian random variables subject to these global symmetries. The external field $\Omega(\mu_f, T)$ representing temperature and chemical potentials is introduced according to the following criteria:

- The chemical potential breaks the global flavor symmetry in the same way as in the QCD partition function.
- The temperature field does not break global flavor symmetries.
- For an anti-hermitian Dirac operator, the temperature field is anti-hermitian, whereas the chemical potential field is hermitian.

- The eigenvalues of the external field are $\mu_f \pm inT$. In this article we only consider the case $n = 1$.

For two flavors, the Dirac operator of the random matrix model is given by

$$\begin{pmatrix} m_1 & \lambda & W + \omega(T) + \mu_1 & 0 \\ -\lambda & m_2 & 0 & W + \omega(T) + \mu_2 \\ -W^\dagger + \omega(T) + \mu_1 & 0 & m_1 & -\lambda \\ 0 & -W^\dagger + \omega(T) + \mu_2 & \lambda & m_2 \end{pmatrix}. \quad (3.1)$$

We have also included a pion condensate source term, which in QCD is given by

$$i\lambda\bar{\psi}\gamma_5\tau_2\psi, \quad (3.2)$$

where the Pauli matrix τ_2 acts in flavor space. The matrix elements of the $n \times n$ matrix W are complex with probability distribution given by

$$P(W) = \exp(-nG^2\text{Tr}WW^\dagger). \quad (3.3)$$

The temperature field given by the matrix

$$\omega(T) = \begin{pmatrix} iT & 0 \\ 0 & -iT \end{pmatrix} \quad (3.4)$$

includes only the two lowest Matsubara frequencies. At zero chemical potentials, this temperature dependence will result in a second order phase transition along the temperature axis [45]. If we write the determinant as a Grassmann integral, the partition function of our model is given by

$$Z = \int \mathcal{D}W \prod_f d\psi^f d\bar{\psi}^f P(W) \exp[-\sum_f \bar{\psi}^f D\psi^f] \quad (3.5)$$

where D is the Dirac matrix given in (3.1). In the thermodynamic limit the partition function is a function of m_1 , m_2 , λ , μ_I , μ_B and T , but for brevity we will not display its arguments.

Other types of random matrix models have also been considered [49, 50, 51, 52]. However, none of these models have been studied at nonzero isospin chemical potential. We mention models with a random gauge potential. In that case, the matrix W has the spin and color structure of the usual Dirac operator,

$$W \rightarrow i\sigma_\nu\tau_k A_\nu^k, \quad \sigma_\nu = (-i, \sigma_k) \quad (3.6)$$

but with A_μ^k a Gaussian $n \times n$ random matrix. Such types of Dirac operators have the same spectral properties [53] as the Dirac operator in (3.5) and lead to a similar phase diagram.

IV. EFFECTIVE PARTITION FUNCTION

Because of the unitary invariance of the random matrix models, the partition function can be rewritten in terms of invariant degrees of freedom only. Below we rewrite the partition functions introduced in Section III in terms of these effective degrees of freedom.

We consider the random matrix model for QCD at nonzero temperature, baryon and isospin chemical potentials given in (3.5). The Gaussian integration over the matrix elements of W can be performed trivially. The resulting four-fermion interaction is decoupled by means of a Hubbard-Stratonovich transformation at the expense of introducing mesonic degrees of freedom. After performing the Grassmann integrations, the partition function (3.5) can thus be written as

$$Z = \int \mathcal{D}A \exp(-\mathcal{L}(A, A^\dagger)), \quad (4.1)$$

where

$$\begin{aligned} \mathcal{L} &= nG^2\text{Tr}(A - M^\dagger)(A^\dagger - M) - \frac{n}{2}\text{Tr} \log Q' \\ &= nG^2\text{Tr}(A - M^\dagger)(A^\dagger - M) - \frac{n}{2}\text{Tr} \log Q^\dagger Q, \end{aligned} \quad (4.2)$$

and A is an arbitrary complex $N_f \times N_f$ matrix. The determinant of the $4N_f \times 4N_f$ matrix Q' , given by

$$\begin{vmatrix} A & 0 & iT + \mu_B + \mu_I I_3 & 0 \\ 0 & A & 0 & -iT + \mu_B + \mu_I I_3 \\ iT + \mu_B + \mu_I I_3 & 0 & A^\dagger & 0 \\ 0 & -iT + \mu_B + \mu_I I_3 & 0 & A^\dagger \end{vmatrix}, \quad (4.3)$$

with $I_3 = \text{diag}(1, -1)$, factors into the determinant of

$$Q = \begin{pmatrix} A & iT + \mu_B + \mu_I I_3 \\ iT + \mu_B + \mu_I I_3 & A^\dagger \end{pmatrix} \quad (4.4)$$

and its Hermitian conjugate. The mass matrix is given by

$$M = \begin{pmatrix} m_1 & -\lambda \\ \lambda & m_2 \end{pmatrix}. \quad (4.5)$$

By shifting A , we have absorbed the dependence on M into the quadratic term.

At zero temperature and chemical potentials, the chiral random matrix partition function is equivalent to the zero momentum part of the QCD chiral Lagrangian. We will now show that this is also the case for the chiral Lagrangian that can be derived from (4.1). To derive this result, we use the power counting scheme that is used in the construction of the chiral Lagrangian: μ_I , $m_\pi \sim \sqrt{m}$ and $\sqrt{\lambda}$ are of the same order [16]. We thus expand the Random Matrix Theory effective Lagrangian to first order in m and λ and second order in μ_I about the saddle

point obtained for $\mu_I = m = \lambda = 0$. The saddle point equation given by

$$G^2((AA^\dagger + T^2 - \mu_B^2)^2 + 4\mu_B^2 T^2)A = (AA^\dagger + T^2 - \mu_B^2)A \quad (4.6)$$

has two solutions,

$$A = 0, \quad (4.7)$$

or the solution of

$$G^2((AA^\dagger + T^2 - \mu_B^2)^2 + 4\mu_B^2 T^2) = (AA^\dagger + T^2 - \mu_B^2). \quad (4.8)$$

For $\mu_I = 0$ it is a natural assumption that the flavor symmetry is not spontaneously broken. We can parameterize A in the broken phase as

$$A = \frac{1}{G}\bar{\sigma}(\mu_B, T)\Sigma, \quad (4.9)$$

where Σ is a unitary matrix and

$$\bar{\sigma}(\mu_B, T) = \left(\frac{1}{2} + \frac{1}{2}\sqrt{1 - (4G^2\mu_B T)^2 - T^2 G^2 + \mu_B^2 G^2} \right)^{1/2} \quad (4.10)$$

is a solution of the saddle point equation (4.8). Using the ansatz (4.9), the inverse of the matrix Q for $\mu_I = 0$ is given by

$$Q^{-1} = \frac{1}{\bar{\sigma}^2/G^2 - (\mu_B + iT)^2} \begin{pmatrix} A^\dagger & -\mu_B - iT \\ -\mu_B - iT & A \end{pmatrix}. \quad (4.11)$$

Inserting this result and the parameterization (4.9) in the chiral expansion of the Lagrangian (4.2), one easily derives

$$\begin{aligned} \mathcal{L} = & c_0(\mu_B, \mu_I, T) - nG\bar{\sigma}(\mu_B, T)\text{Tr}(M\Sigma^\dagger + M^\dagger\Sigma) \\ & + n\mu_I^2 G^2 \bar{\sigma}^2(\mu_B, T)c_2(\mu_B, T)\text{Tr}(\Sigma^\dagger I_3 \Sigma I_3), \end{aligned} \quad (4.12)$$

where $c_0(\mu_B, \mu_I, T)$ is independent of Σ and

$$c_2(\mu_B, T) = \left(1 - \frac{(4G^2\mu_B T)^2}{4(\bar{\sigma}^2(\mu_B, T) - G^2(\mu_B^2 - T^2))^2} \right). \quad (4.13)$$

This effective Lagrangian coincides with the zero momentum part of the leading-order Chiral Lagrangian at zero temperature and baryon chemical potential derived in [17, 18] based on the symmetries of QCD. A transition to a pion condensation phase takes place at $\mu_{I,c}^2 = m/(2G\bar{\sigma}(\mu_B, T)c_2(\mu_B, T))$. The pion condensate vanishes for $\mu_I < \mu_{I,c}$. For $\mu_I > \mu_{I,c}$ the chiral condensate rotates into a pion condensate but the sum of the squares of the chiral condensate and the pion condensate remains constant. The temperature and the baryon chemical potential affect both the magnitude and the orientation of the condensates.

V. PHASE DIAGRAM

As was argued in [15, 16], the free energy (4.12) is completely determined by the transformation properties of the QCD partition function. Since the random matrix model has the same global transformation properties as the QCD partition function, we thus find the same low-energy limit. In this section we analyze the random matrix partition function beyond this universal domain. In our model we will be able to study the partition function to all orders in the mass, chemical potential and temperature. We will show that the inclusion of such non-perturbative contributions alters the nature of the phase transition.

A. Observables

We consider three different observables, the chiral condensates $\langle \bar{u}u \rangle$ and $\langle \bar{d}d \rangle$, and the pion condensate $\frac{1}{2}(\langle \bar{u}\gamma_5 d \rangle - \langle \bar{d}\gamma_5 u \rangle)$. They can be expressed in terms of derivatives of the partition function,

$$\begin{aligned} \langle \bar{u}u \rangle &= \frac{1}{2n}\partial_{m_1} \log Z^{\text{eff}} \\ &= G^2 \left(\frac{1}{2}\langle A_{11}^* + A_{11} \rangle - m_1 \right), \end{aligned} \quad (5.1)$$

$$\begin{aligned} \langle \bar{d}d \rangle &= \frac{1}{2n}\partial_{m_2} \log Z^{\text{eff}} \\ &= G^2 \left(\frac{1}{2}\langle A_{22}^* + A_{22} \rangle - m_2 \right), \end{aligned} \quad (5.2)$$

$$\begin{aligned} &\frac{1}{2}(\langle \bar{u}\gamma_5 d \rangle - \langle \bar{d}\gamma_5 u \rangle) \\ &= \frac{1}{4n}\partial_\lambda \log Z^{\text{eff}} \\ &= G^2 \left(\frac{1}{4}\langle A_{12} + A_{12}^* - A_{21} - A_{21}^* \rangle - \lambda \right). \end{aligned} \quad (5.3)$$

The expectation values of the diagonal matrix elements of A can be interpreted as the chiral condensates, whereas its off-diagonal elements represent the pion condensate.

B. Effective potential

In the large- n limit, the partition function can be calculated by a saddle point approximation. To solve the saddle point equations, we make an ansatz for the matrix A . Since we have two independent chemical potentials, the chiral condensates are not necessarily equal, whereas for a sufficiently large isospin chemical potential we expect a pion condensate. Based on the expressions for the chiral condensate and the pion condensate, we make the following ansatz for A

$$A = \begin{pmatrix} \sigma_1 & \rho \\ -\rho & \sigma_2 \end{pmatrix}. \quad (5.4)$$

In this parameterization, the different condensates are given by $\langle \bar{u}u \rangle = G^2(\sigma_1 - m_1)$, $\langle \bar{d}d \rangle = G^2(\sigma_2 - m_2)$, and $\frac{1}{2}(\langle \bar{u}\gamma_5 d \rangle - \langle \bar{d}\gamma_5 u \rangle) = G^2(\rho - \lambda)$. Using this ansatz, we obtain the effective potential

$$\begin{aligned} \frac{1}{n}\mathcal{L} &= G^2((\sigma_1 - m)^2 + (\sigma_2 - m)^2 + 2(\rho - \lambda)^2) \\ &- \frac{1}{2} \sum_{\pm} \log [((\sigma_1 + (\mu_1 \pm iT))(\sigma_2 - (\mu_2 \pm iT)) + \rho^2) \\ &\times ((\sigma_1 - (\mu_1 \pm iT))(\sigma_2 + (\mu_2 \pm iT)) + \rho^2)]. \end{aligned} \quad (5.5)$$

From here on, we set $m_1 = m_2 = m$. For $\rho = 0$ this effective potential is a function of μ_f^2 . In particular, this means that its dependence on μ_I at $\mu_B = 0$ is the same as its dependence on μ_B at $\mu_I = 0$. This implies that for the critical temperature we have the relation [5, 14]

$$T_c(\mu_I)|_{\mu_B=0} = T_c(\mu_B)|_{\mu_I=0} \quad \text{for } \rho = 0. \quad (5.6)$$

The fermion determinant of the theory with $\mu_B = 0$ and equal quark masses is equal to the fermion determinant of the phase quenched partition function. We thus expect that the phase quenched approximation works in the phase where the pion condensate vanishes.

To find the phase structure of our partition function, we have to solve the saddle point equations

$$\frac{\partial \mathcal{L}}{\partial \sigma_1} = 0, \quad \frac{\partial \mathcal{L}}{\partial \sigma_2} = 0, \quad \frac{\partial \mathcal{L}}{\partial \rho} = 0. \quad (5.7)$$

We will treat the following cases analytically: the chiral limit ($m = 0$) at zero T and at finite T , and the case $m \neq 0$ at $T = 0$. We will calculate the phase diagram for $T \neq 0$ and $m \neq 0$ by numerically minimizing the effective potential. In addition, some analytical results are obtained for large quark mass m .

C. Chiral limit at $T = 0$

In the case of vanishing quark mass, zero diquark source, and zero temperature, the effective potential simplifies to

$$\begin{aligned} \frac{1}{n}\mathcal{L} &= G^2(\sigma_1^2 + \sigma_2^2 + 2\rho^2) \\ &- \frac{1}{2} \log ((\sigma_1 + \mu_1)(\sigma_2 - \mu_2) + \rho^2)^2 \\ &- \frac{1}{2} \log ((\sigma_1 - \mu_1)(\sigma_2 + \mu_2) + \rho^2)^2. \end{aligned} \quad (5.8)$$

In the chiral limit, chiral symmetry is broken spontaneously. As soon as the isospin chemical potential is switched on, the chiral condensate rotates into a pion condensate. Therefore, no phase exists where both condensates are nonzero. The saddle point equation for ρ has two possible solutions: $\rho = 0$ and $\rho \neq 0$. We first consider the case $\rho = 0$.

For $\rho = 0$, the effective potential separates into the sum of free energies for σ_1 and σ_2 ,

$$\frac{1}{n}\mathcal{L} = \sum_{f=1,2} G^2 \sigma_f^2 - \frac{1}{2} \log(\sigma_f^2 - \mu_f^2)^2. \quad (5.9)$$

The saddle point equations given by

$$\sigma_f (G^2(\sigma_f^2 - \mu_f^2) - 1) = 0, \quad f = 1, 2, \quad (5.10)$$

have the solutions

$$\sigma_f = 0, \quad f = 1, 2, \quad (5.11)$$

$$\sigma_f^2 = \frac{1}{G^2} + \mu_f^2, \quad f = 1, 2. \quad (5.12)$$

The contribution to the free energy from one flavor for these solutions is given by

$$\Omega_f = -\log \mu_f^2, \quad (5.13)$$

$$\Omega_f = 1 + \log G^2 + \mu_f^2 G^2, \quad (5.14)$$

respectively. The full free energy is a sum over the contributions from both flavors. The two solutions are separated by a first order phase transition line where their free energy is equal,

$$1 + \mu_f^2 G^2 + \log(\mu_f^2 G^2) = 0. \quad (5.15)$$

The solution of this transcendental equation is given by $\mu_f G = \mu_c G \approx 0.527697$ [46]. At this point a first order phase transition to a phase with $\sigma_f = 0$ takes place. In the μ_1 - μ_2 -plane, we can thus distinguish four different phases with nonzero condensates in strips along the chemical potential axes. The strips overlap in the center and form a region where both chiral condensates are nonzero.

At zero quark mass, the Goldstone bosons are massless, and the critical value of the chemical potential for pion condensation is $\mu_I = 0$. For $\mu_I > 0$, the chiral condensates rotate completely into a pion condensate, so that $\sigma_1 = \sigma_2 = 0$. The effective potential for ρ is given by

$$\frac{1}{n}\mathcal{L} = 2G^2 \rho^2 - \log(\rho^2 - \mu_1 \mu_2)^2. \quad (5.16)$$

The saddle point equation given by

$$\rho(G^2(\rho^2 - \mu_1 \mu_2) - 1) = 0 \quad (5.17)$$

has again two solutions,

$$\begin{aligned} \rho &= 0, \\ \rho^2 &= \frac{1}{G^2} + \mu_1 \mu_2. \end{aligned} \quad (5.18)$$

A second order transition line is given by the hyperbola $\rho^2 = 0$ in the quadrants where $\mu_1 \mu_2 < 0$. The free energy of this phase is given by

$$\Omega_\rho = 2(1 + \log G^2 + \mu_1 \mu_2 G^2). \quad (5.19)$$

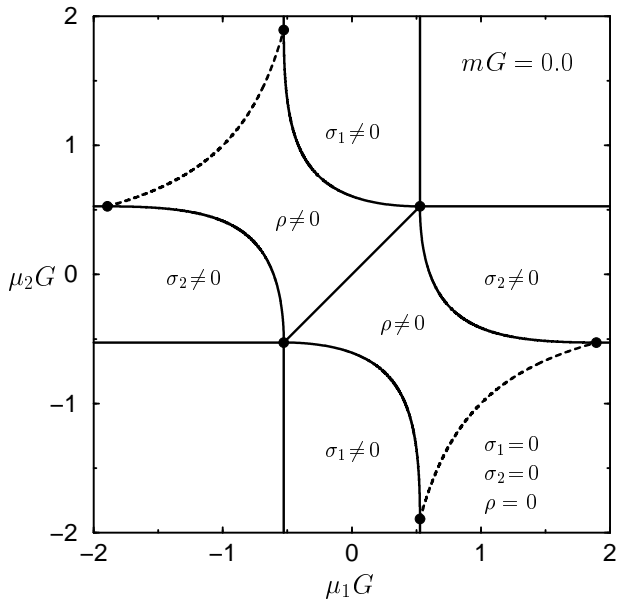


FIG. 1: Phase diagram of the RMT model for three colors in the chiral limit ($m = 0$) at zero temperature. Solid (dashed) lines are lines of first (second) order phase transitions. Except for the four corner regions, the different phases are marked by the nonvanishing condensate. In the four corner regions we have that $\rho = \sigma_1 = \sigma_2 = 0$.

Finally, for $\mu_1 = \mu_2$, the saddle point equations allow a solution with $\rho \neq 0$ and $\sigma_1 = \sigma_2 \neq 0$. However, the free energy of this solution is higher than that of the solution with $\sigma_1 = \sigma_2 \neq 0$ and $\rho = 0$. Physically this is clear, since the pion condensate is expected to vanish for zero isospin chemical potential.

Comparing the free energy of the pion condensation phase to those of the chiral condensation phases and the chiral restored phase, we can determine the remaining first order phase transition lines. The resulting phase diagram is shown in Fig. 1. We find a region of pion condensation in the center of the phase diagram. It is bounded by first order phase transitions towards phases with nonzero chiral condensate for one flavor, and by second order transition lines towards the chiral restored phase. The chiral condensation phases form the arms of a cross along the chemical potential axes. Since σ_1 is independent of μ_2 , it is nonzero in a strip along the μ_2 -axis, and the same applies for the other flavor. The first order lines intersect in the two points $(\mu_1 G, \mu_2 G) \approx (\pm 0.527697, \pm 0.527697)$. The intersection points of the second order lines with the first order transitions between the pion and chiral condensation phases are at $(\mu_1 G, \mu_2 G) \approx (\pm 0.527697, \mp 1.895025)$, and at the two points obtained by interchanging the values for μ_1 and μ_2 .

D. Chiral limit at $T \neq 0$

At nonzero temperature, we analyze the phase structure in the same way as we did for $T = 0$, and, initially, we also find the same phases.

In a phase with vanishing pion condensate, the effective potential again separates into a sum over contributions of two different flavors,

$$\frac{1}{n}\mathcal{L} = \sum_{f=1,2} G^2 \sigma_f^2 - \frac{1}{2} \log((\sigma_f^2 - \mu_f^2 + T^2)^2 + 4\mu_f^2 T^2). \quad (5.20)$$

This free energy was studied in [11] for the case of zero isospin chemical potential. For each of the two flavors ($f = 1, 2$), the saddle point equation

$$\sigma_f \left(\sigma_f^4 - 2\left(\frac{1}{2G^2} + \mu_f^2 - T^2\right)\sigma_f^2 + \frac{\mu_f^2 - T^2}{G^2} + (\mu_f^2 + T^2)^2 \right) = 0 \quad (5.21)$$

has the solutions

$$\begin{aligned} \sigma_f &= 0, \\ \sigma_f^2 &= \frac{1}{2G^2} + \mu_f^2 - T^2 \pm \frac{1}{2G^2} \sqrt{1 - (4G^2 \mu_f T)^2}. \end{aligned} \quad (5.22)$$

The free energy for each flavor of these solutions is equal to

$$\begin{aligned} \Omega_f &= -\log(\mu_f^2 + T^2), \\ \Omega_f &= \frac{1}{2} + \log G^2 + G^2(\mu_f^2 - T^2) \pm \frac{1}{2} \sqrt{1 - (4G^2 \mu_f T)^2} \\ &\quad - \frac{1}{2} \log \left(\frac{1}{2} \pm \frac{1}{2} \sqrt{1 - (4G^2 \mu_f T)^2} \right), \end{aligned} \quad (5.23)$$

respectively. For $(4G^2 \mu_f T)^2 < 1$, the solution with the negative branch of the square root will be discarded, since it does not minimize the free energy. The second order phase transition line is given by the condition that the two solutions coincide. One easily derives

$$(\mu_f^2 - T^2) + G^2(\mu_f^2 + T^2)^2 = 0. \quad (5.25)$$

Since there is always the solution $\sigma_f = 0$, there can be a first order transition when the coefficient of σ_f^3 in the saddle point equation (5.21) becomes negative. A tricritical point occurs where both the coefficient of σ_f and σ_f^3 in (5.21) vanish. This results in the equations

$$\begin{aligned} \frac{1}{2G^2} + \mu_f^2 - T^2 &= 0, \\ \mu_f^2 - T^2 + G^2(\mu_f^2 + T^2)^2 &= 0, \end{aligned} \quad (5.26)$$

with solution given by

$$\begin{aligned} \mu_{f,3}^2 G^2 &= \frac{\sqrt{2}-1}{4}, \quad f = 1, 2, \\ T_3^2 G^2 &= \frac{\sqrt{2}+1}{4}. \end{aligned} \quad (5.27)$$

Numerically, $T_3G \approx 0.776887$, $\mu_{f,3}G \approx 0.321797$, which was also obtained in [11].

In Fig. 2, we show the phase diagram for fixed temperature in the μ_1 - μ_2 chemical potential plane. The transition lines for each flavor are straight and constant in the chemical potential for the other flavor. In this plane, the phase transition lines change in their entirety from first to second order when we pass the tricritical temperature (5.27) from below. The critical chemical potential of the transition becomes smaller with increasing temperature. A baryon chemical potential that is large enough will destroy the pion condensate.

Since the two chiral condensates are independent of one another and depend only on the chemical potential for the respective flavor, we again have four phases. A phase where chiral symmetry is restored ($\sigma_1 = \sigma_2 = 0$), and phases where either one or both of the chiral condensates are nonzero. The free energies are simply given by the sum of the one-flavor free energies.

At nonzero isospin chemical potential, we expect that in the limit of massless quarks the chiral condensates are completely rotated into a pion condensate. The effective potential for vanishing σ_f and nonzero pion condensate ρ becomes

$$\frac{1}{n}\mathcal{L} = 2G^2\rho^2 - \log((\rho^2 - \mu_1\mu_2 + T^2)^2 + T^2(\mu_1 + \mu_2)^2). \quad (5.28)$$

The saddle point equation reads

$$G^2\rho\left(\rho^4 - 2\left(\frac{1}{2G^2} + \mu_1\mu_2 - T^2\right)\rho^2 + \frac{1}{G^2}(\mu_1\mu_2 - T^2) + (\mu_1\mu_2 - T^2)^2 + T^2(\mu_1 + \mu_2)^2\right) = 0. \quad (5.29)$$

It has the solutions

$$\begin{aligned} \rho &= 0, \\ \rho^2 &= \frac{1}{2G^2} + \mu_1\mu_2 - T^2 \pm \frac{1}{2G^2}\sqrt{1 - (2G^2(\mu_1 + \mu_2)T)^2}. \end{aligned} \quad (5.30)$$

Again the solution with the negative branch of the square root has a larger free energy. A line of second order phase transitions is determined by the condition that the two solutions coincide:

$$(\mu_1\mu_2 - T^2) + G^2(\mu_1\mu_2 - T^2)^2 + G^2T^2(\mu_1 + \mu_2)^2 = 0. \quad (5.31)$$

A first order phase transition may occur when the coefficient of ρ^3 in (5.29) vanishes. However, we will see below that this happens in a region where solutions with nonzero chiral condensate have a lower free energy.

In Fig. 2 we show the phase diagram in the μ_1 - μ_2 -plane for zero quark mass and temperatures equal to $TG = 0.3$, $TG = 0.5$, $TG = 0.6$ and $TG = 0.8$. The first order lines in the phase diagram are obtained by combining the results for the free energies of the phases discussed above.

The phase diagram at $T = 0$ has been described in the previous section. With increasing temperature, the second order transition between the pion condensation phase and the chiral restored phase moves towards the origin. The effect of the temperature term on the phase diagram is a shrinking of the condensate phases. The critical chemical potential for the chiral restoration transition decreases with temperature, so that the transition lines move toward the axes as well.

At lower temperatures, the phase where both chiral condensates are nonzero simultaneously is always higher in energy than the pion condensation phase, and consequently it is not realized. At a temperature of $TG \approx 0.548047$, a first order transition between the pion condensation phase and the phase with $\sigma_1 \neq 0$, $\sigma_2 \neq 0$, and $\rho = 0$ emerges, and it appears at the intersection points of the first order transitions, $\mu_1G = \mu_2G \approx 0.413485$, around the line $\mu_1 = \mu_2$. The upper boundaries of this phase are always the transition lines where either of the two chiral condensates vanish.

The position of the tricritical point in the μ_f - T -plane for any of the two chiral condensates σ_f is unaffected by the presence of the second chemical potential. Therefore, we find that at a temperature $T_3G = \frac{1}{2}\sqrt{\sqrt{2} + 1} \approx 0.776887$, the phase transition lines between the chiral condensed phases and the chiral restored phase in the chemical potential plane become second order transition lines in their entirety.

Above this temperature, the regions with nonzero chiral condensates along the μ_1 - and μ_2 -axes are bounded by second order transition lines to the chiral restored phase. We can observe the region where both phases with chiral condensation overlap. The pion condensation phase in the center is separated from the chiral condensation phases by first order transition lines, and from the chiral restored phase by a second order transition line.

All condensation phases vanish at the same temperature $TG = 1$.

E. Zero temperature limit at nonzero quark mass

Away from the chiral limit, we can only solve the saddle point equation analytically for $T = 0$. The results of this particular case will be discussed in this section. The phase diagram at nonzero quark mass is qualitatively different from the phase diagram in the chiral limit. First, the chiral condensates, σ_1 and σ_2 , are not good order parameters anymore, and, second, we expect a phase transition to a phase with nonzero pion condensate for $\mu_I = m_\pi/2$. However, in this case the chiral condensates are non-vanishing in the phase with $\rho \neq 0$.

The effective potential is given by

$$\begin{aligned} \frac{1}{n}\mathcal{L} &= G^2((\sigma_1 - m)^2 + (\sigma_2 - m)^2 + 2\rho^2) \\ &\quad - \frac{1}{2}\log((\sigma_1 + \mu_1)(\sigma_2 - \mu_2) + \rho^2)^2 \end{aligned}$$

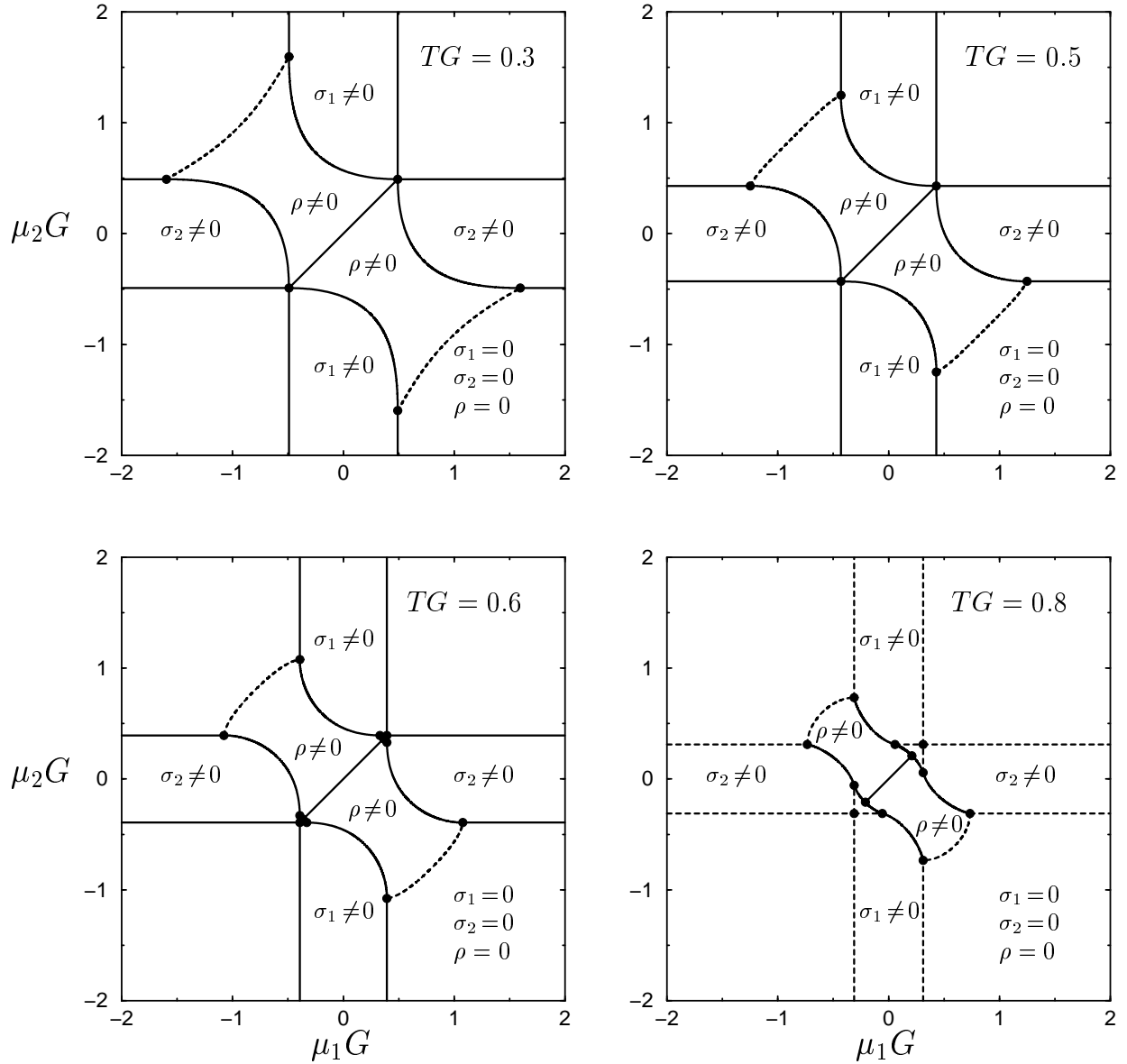


FIG. 2: Phase diagram of the RMT model in the chiral limit for different temperatures. Solid (dashed) lines are lines of first (second) order transitions. The values for the temperature are given in the figures. Except for the four corner regions, the phases are marked by condensates that do not vanish in the chiral limit. In the four corner regions we have that $\rho = \sigma_1 = \sigma_2 = 0$. For $TG = 0.6$, the phase with $\sigma_1 \neq 0$, $\sigma_2 \neq 0$ has emerged. For $TG = 0.8$, the chiral restoration transitions have become second order transitions. The region in the center where both chiral condensation phases overlap and the chiral condensates for both flavors are nonzero can be seen clearly. All condensates vanish at $TG = 1$.

$$-\frac{1}{2} \log ((\sigma_1 - \mu_1)(\sigma_2 + \mu_2) + \rho^2)^2. \quad (5.32)$$

Obviously, it is symmetric under a simultaneous interchange of the chiral condensates σ_1 and σ_2 and the two chemical potentials μ_1 and μ_2 . The saddle point equations are given by

$$2G^2(\sigma_1 - m) = \frac{\sigma_2 - \mu_2}{(\sigma_1 + \mu_1)(\sigma_2 - \mu_2) + \rho^2} + \frac{\sigma_2 + \mu_2}{(\sigma_1 - \mu_1)(\sigma_2 + \mu_2) + \rho^2}, \quad (5.33)$$

$$2G^2(\sigma_2 - m) = \frac{\sigma_1 + \mu_1}{(\sigma_1 + \mu_1)(\sigma_2 - \mu_2) + \rho^2} + \frac{\sigma_1 - \mu_1}{(\sigma_1 - \mu_1)(\sigma_2 + \mu_2) + \rho^2}, \quad (5.34)$$

$$2G^2\rho = \frac{\rho}{(\sigma_1 + \mu_1)(\sigma_2 - \mu_2) + \rho^2} + \frac{\rho}{(\sigma_1 - \mu_1)(\sigma_2 + \mu_2) + \rho^2}. \quad (5.35)$$

As we see from the last equation in (5.35), there is always a solution with $\rho = 0$. We expect that this is the actual

minimum of the free energy below the critical chemical isospin potential for pion condensation. In this case, as for $m = 0$, the saddle point equations for the two chiral condensates decouple and are given by

$$G^2(\sigma_f - m)(\sigma_f^2 - \mu_f^2) - \sigma_f = 0. \quad (5.36)$$

Although this third-order equation can be solved analytically, it is more instructive to expand it in powers of m . To first order in m , we find for σ_f , $f = 1, 2$,

$$\begin{aligned} \sigma_f &= \pm \frac{1}{G} \left(\sqrt{1 + \mu_f^2 G^2} + \frac{mG}{2(1 + \mu_f^2 G^2)} + \mathcal{O}(m^2 G^2) \right) \\ &= \pm \frac{1}{G} \left(1 + \frac{1}{2} \mu_f^2 G^2 + \frac{1}{2} mG + \mathcal{O}(m^2 G^2, \mu_f^4 G^4) \right), \end{aligned} \quad (5.37)$$

$$\sigma_f = \frac{\mu_f^2 G^2}{1 + \mu_f^2 G^2} m + \mathcal{O}(m^3 G^2). \quad (5.38)$$

The free energy of these solutions is given by

$$\Omega_f = 1 + \log G^2 + \mu_f^2 G^2 - 2mG + \mathcal{O}(m^2 G^2), \quad (5.39)$$

$$\Omega_f = -\log(\mu_f^2) - \mathcal{O}(m^2 G^2), \quad (5.40)$$

respectively. The solutions (5.37) minimize the free energy for small values of the chemical potential, and the solution (5.38) minimizes the free energy for large values of the chemical potential. As in the chiral limit, we once again have four phases, where either chiral symmetry is broken spontaneously and the chiral order parameters $G\sigma_f$ are of $\mathcal{O}(1)$, or where it is broken only explicitly and the chiral order parameters are of the order of the quark mass, $\mathcal{O}(m)$. The free energies in these cases are given by the sum of the free energies for each flavor. In contrast to the case of the chiral limit $m = 0$, the phase with $\sigma_1 \neq 0$, $\sigma_2 \neq 0$ appears at the center of the phase diagram.

By matching the free energies for the phases with large and small values of the chiral condensates, we obtain the correction to the critical chemical potential due to the finite quark mass m . The critical chemical potential shifts to

$$\mu'_{f,c} G = \mu_c G \left(1 + \frac{mG}{1 + \mu_c^2 G^2} + \mathcal{O}(m^2 G^2) \right), \quad (5.41)$$

where $\mu_c G$ is the result for the chiral limit, obtained in (5.15).

For $m \neq 0$, both the pion condensate as well as the chiral condensates are nonzero in the phase with $\rho \neq 0$. We have to solve the full system of three saddle point equations. In fact, in this case the analytical solution is relatively simple. The two chiral condensates are related by the equation

$$\sigma_1 - \sigma_2 = m \frac{\mu_1 + \mu_2}{\mu_1 - \mu_2}. \quad (5.42)$$

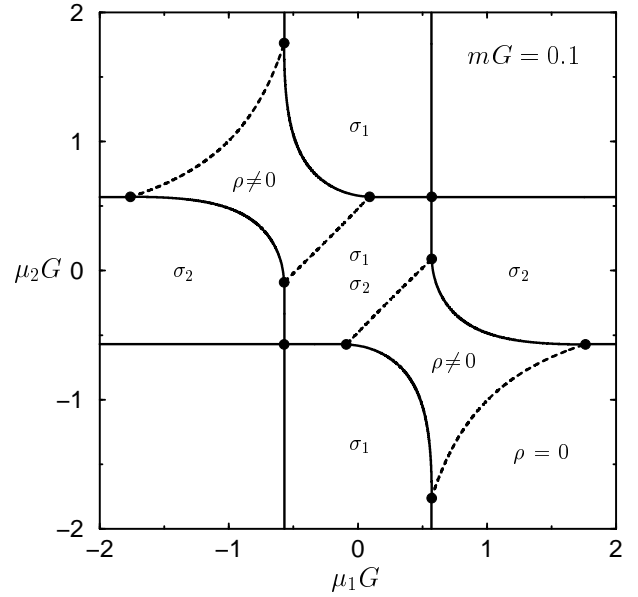


FIG. 3: Phase diagram of the RMT model for three colors at a value of the quark mass of $mG = 0.1$. Solid (dashed) lines are lines of first (second) order transitions. Except for the four corner regions, the different phases are marked by the condensate that does not vanish in the chiral limit. The condensates that are not displayed are of $\mathcal{O}(m)$. In the four corner regions we have that $\rho = 0$, $\sigma_1 = \mathcal{O}(m)$ and $\sigma_2 = \mathcal{O}(m)$.

The solution for σ_f , $f = 1, 2$, is given by

$$\sigma_f = m\mu_f \frac{\mu_1 + \mu_2}{(\mu_1 - \mu_2)^2} + \frac{2m}{G^2} \frac{1}{(\mu_1 - \mu_2)^2 - 4m^2}. \quad (5.43)$$

The pion condensate then follows from

$$(\sigma_1 - m)(\sigma_2 - m) + \rho^2 = \frac{1}{G^2} + \mu_1 \mu_2 - 4 \frac{m^2 \mu_1 \mu_2}{(\mu_1 - \mu_2)^2}. \quad (5.44)$$

The free energy of this solution is

$$\begin{aligned} \Omega(m, \mu_1, \mu_2) &= 2 \left(1 + \log G^2 + \mu_1 \mu_2 G^2 + m^2 G^2 \right) \\ &\quad - m^2 G^2 \frac{(\mu_1 + \mu_2)^2}{(\mu_1 - \mu_2)^2} \\ &\quad - \frac{1}{2} \log \left(\frac{(\mu_1 - \mu_2)^2}{(\mu_1 - \mu_2)^2 - 4m^2} \right). \end{aligned} \quad (5.45)$$

For nonzero quark mass m , the phase in which $\rho \neq 0$ does not extend to zero isospin chemical potential. For $\mu_B = 0$, the onset chemical potential follows by equating the free energy $\Omega_1 + \Omega_2$ of (5.39) to the free energy of the pion condensed phase given in eq. (5.45). It is given by $\mu'_{1,c} = \frac{m}{2G} + \mathcal{O}(m^2)$ which identifies $\sqrt{2m/G}$ as the pion mass for $\mu_B = T = 0$.

By putting $\rho^2 = 0$ in eq. (5.44), we obtain the complete second order transition line that bounds the pion

condensation phase at low as well as high isospin chemical potential. Parametrized in terms of the baryon and isospin chemical potentials, it is given by

$$\left(\frac{\mu_B^2 - \mu_I^2}{4\mu_I^2} + \frac{1}{2G^2} \frac{m}{\mu_I^2 - m^2}\right) m^2 \frac{\mu_B^2}{\mu_I^2} - \mu_B^2 + \mu_I^2 - \frac{1}{G^2} \frac{\mu_I^2}{\mu_I^2 - m^2} + \frac{m^2}{4G^4} \frac{1}{(\mu_I^2 - m^2)^2} = 0. \quad (5.46)$$

For $\mu_B = 0$ we again find a critical chemical potential given by $\mu_{I,c} = m/2G + \mathcal{O}(m^2)$. The phase diagram in the μ_1 - μ_2 -plane for $mG = 0.1$ and zero temperature is shown in Fig. 3. The qualitative difference to the massless case is the appearance of a region where both chiral condensates are nonzero in the center of the phase diagram. The dashed lines that border this region cross the μ_I -axis ($\mu_B = 0$) at $\mu_I = \pm m\pi/2$ and are roughly constant in μ_B . They coincide in the chiral limit, and the central region becomes a phase of nonzero pion condensate and zero chiral condensates (see Fig. 1). For small quark masses m , the phase diagram at large values of the chemical potentials is almost unchanged in comparison to the phase diagram we found in the chiral limit. The transition lines are only shifted by small corrections of the order of the mass mG .

F. Phase diagram at nonzero quark mass and temperature

Finally, we study the phase diagram at nonzero quark mass and temperature. In this case it is no longer possible to obtain an analytical solution of the saddle point equations. Instead, we determine the minimum of the free energy numerically. The results for the phases in the μ_1 - μ_2 -plane for temperatures of $TG = 0.3$, $TG = 0.5$, $TG = 0.6$, $TG = 0.8$ are shown in Fig. 4. The quark mass used here is $mG = 0.1$. Below the critical temperature, the phases are the same as at zero temperature (see Fig. 3) and differ qualitatively from the chiral limit only in the central region (see Fig. 2).

The phase diagram in the μ_B - T -plane for $\mu_I = 0$ has been studied in [11]. In the chiral limit, the chiral restoration transition extends as a second order line from the $\mu_B = 0$ axis, changes order at a tricritical point, and intersects the $T = 0$ axis as a line of first order transitions. For nonzero quark mass, the first order transition ends in a critical point, and the second order transition becomes a crossover.

Fig. 5 shows the phase diagram in the μ_B - T -plane at finite quark mass $mG = 0.1$ for zero isospin chemical potential and for $\mu_I G = 0.1$. We observe that the first order curve splits into two first order curves that are separated by $2\mu_I G$. This can be understood as follows. Below the threshold for pion condensation, the free energy separates into a sum over the two flavors. For $\mu_I = 0$, the chiral phase transition lines for both flavors coincide. A finite isospin chemical potential breaks the flavor symme-

try, and the first order transition lines for the two flavors split and shift according to

$$\begin{aligned} \mu_{B,c}^{(1)}(T) &= \mu_c(T) - \mu_I \\ \mu_{B,c}^{(2)}(T) &= \mu_c(T) + \mu_I, \end{aligned} \quad (5.47)$$

where $\mu_c(T)$ describes the transition line at $\mu_I = 0$. The critical temperature is not affected by the isospin chemical potential.

We have seen in eq. (5.6) that in the phase with zero pion condensate the dependence of the critical temperature on the isospin chemical potential at zero baryon chemical potential is the same as the dependence of the critical temperature on the baryon chemical potential at zero isospin chemical potential. This suggests the possibility that for large values of the pion mass a tricritical point may appear in the $\mu_B = 0$ plane. As we will see below, this turns out not to be the case. We first determine the domain in the $\mu_B = 0$ plane where pion condensation occurs.

Performing a similar analysis as below eq. (5.41) for the free energy at $\mu_B = 0$ but nonzero m , T and μ_I , we find that the region of nonzero pion condensate is bounded by the curve

$$\mu_I^2(\mu_I^2 - m^2)G^2 - \frac{1}{4}m^2 - (\mu_I^2 + T^2)(\mu_I^2 - m^2)^2G^4 = 0. \quad (5.48)$$

For asymptotically large values of the quark mass, this curve reduces to the two expressions,

$$\begin{aligned} \mu_{Ic}^2(T)G^2 &= m^2G^2 + \frac{1}{2} \pm \frac{1}{2mG} \sqrt{\frac{1}{2} - T^2G^2} \\ &+ \frac{1}{8m^2G^2}(1 - 4T^2G^2) + \mathcal{O}\left(\frac{1}{m^3G^3}\right). \end{aligned} \quad (5.49)$$

However, for $\mu_B = 0$ the saddle point equations are also solved by $\rho = 0$. Then a first order transition takes place between the solutions with large mass expansion given by

$$\sigma_1 = \sigma_2 = m \pm \frac{1}{G} \sqrt{\frac{1}{2} - G^2T^2} + \mathcal{O}\left(\frac{1}{mG}\right). \quad (5.50)$$

At the tricritical point these solutions merge with the extremum between them. From this condition we find that the position of the tricritical point is given by

$$\begin{aligned} T_3^2G^2 &= \frac{1}{2} - \frac{1}{16m^2G^2} + \mathcal{O}\left(\frac{1}{m^3G^3}\right) \\ \mu_{B,3}^2G^2 &= m^2G^2 + \frac{1}{2} - \frac{1}{8m^2G^2} + \mathcal{O}\left(\frac{1}{m^3G^3}\right), \end{aligned} \quad (5.51)$$

and the value of σ at the tricritical point is equal to

$$\sigma_3 = \frac{1}{4mG^2} + \mathcal{O}\left(\frac{1}{m^2G^2}\right). \quad (5.52)$$

One easily verifies from (5.49) that up to order $1/m^2G^2$ the tricritical point is inside the pion condensation region, where the phase with a nonzero pion condensate is favored. Numerically, one finds that this is also the case for quark masses that are not asymptotically large.

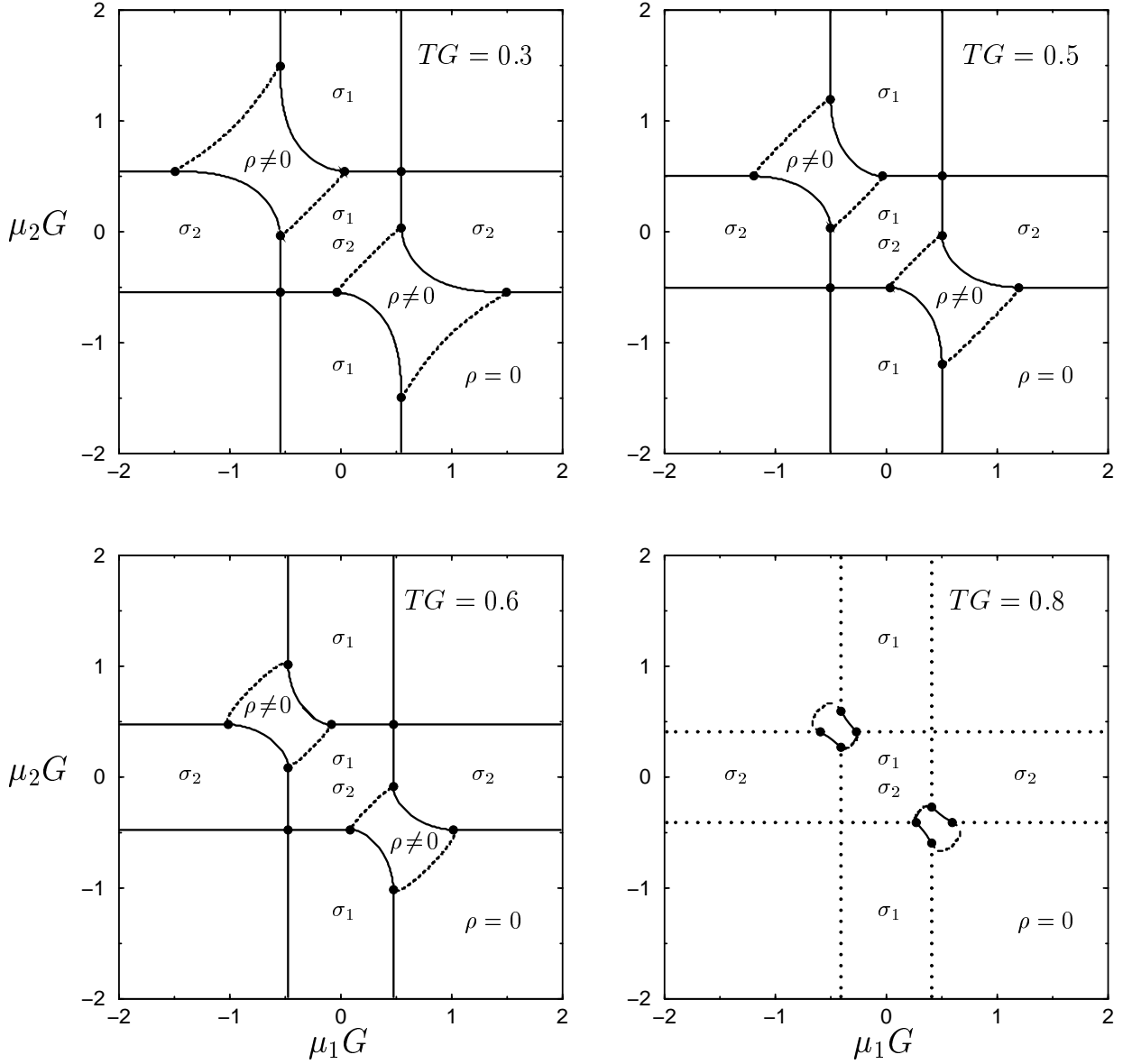


FIG. 4: Phase diagram of the RMT model for three colors for a value of the quark mass of $mG = 0.1$. Values for the temperature are given in the figures. Solid (dashed) lines are lines of first (second) order transitions. Above the critical temperature, the chiral restoration transition becomes a crossover, denoted by dotted lines. Except for the four corner regions, the different phases are marked by the condensate that does not vanish in the chiral limit. The chiral condensates are not displayed when they are of $\mathcal{O}(m)$. In the four corner regions we have that $\rho = 0$, $\sigma_1 = \mathcal{O}(m)$ and $\sigma_2 = \mathcal{O}(m)$.

VI. DISCUSSION

Starting from a random matrix model at nonzero temperature and chemical potential for baryon number and isospin, we have obtained an effective potential for the matrix valued order parameter field. This order parameter field arises naturally in this random matrix model that is based on the global symmetries of the QCD partition function. The expectation value of its diagonal elements are the chiral condensates $\langle \bar{u}u \rangle$ and $\langle \bar{d}d \rangle$, whereas its off-diagonal elements give the pion condensate. To first order in m_π^2 and μ_I^2 and zero baryon chemical poten-

tial and temperature, the random matrix model coincides with the zero momentum part of the chiral Lagrangian that has been derived from QCD. However, the tricritical point found in lattice simulations [34] and in the chiral Lagrangian at nonzero temperature and isospin chemical potential [25] is not present in the random matrix model. We therefore conclude that the pion dynamics are important for the emergence of this tricritical point, as was suggested in [34].

Based on the effective potential, we have obtained a phase diagram for QCD at nonzero temperature, baryon and isospin chemical potentials. We have found a sur-

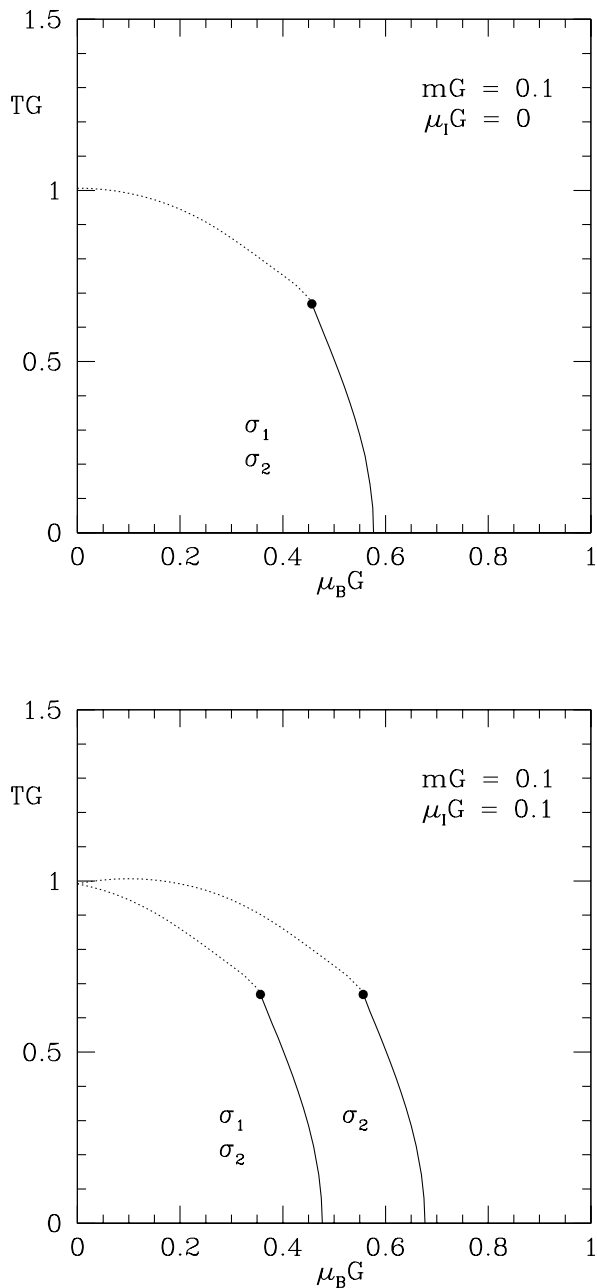


FIG. 5: Phase diagram in the μ_B - T -plane for quark mass $mG = 0.1$ and an isospin chemical as shown in the label of the figure. A first order chiral restoration phase transition takes place at the full line that ends in the critical end point. For nonzero isospin chemical potential (lower figure) this curve is shifted in opposite directions for the chiral restoration transition of $\langle \bar{u}u \rangle$ and $\langle \bar{d}d \rangle$. The condensates that are not displayed are of $\mathcal{O}(m)$. The dotted curves depict the crossover behavior. The temperature of the critical end point is not affected by the isospin chemical potential.

prisingly rich phase diagram characterized by the con-

densates in our order parameter field. We find that close to the critical baryon chemical potential a small isospin chemical potential leads to a phase with $\langle \bar{u}u \rangle$ of the order of Λ_{QCD}^3 but $\langle \bar{d}d \rangle$ reduced by a factor m/Λ_{QCD} .

In the phase with a vanishing pion condensate, the effective potential is an even function of the chemical potentials and separates into a sum of free energies for each of the two flavors. This has important consequences. Since the effective potential is even, the dependence of the partition function on μ_B at $\mu_I = 0$ is the same as its dependence on μ_I at $\mu_B = 0$. Therefore, the phase diagram for baryon chemical potential smaller than the pion mass can be studied reliably by means of the phase quenched partition function. Because of the separability of the free energy, the critical curve for $\mu_I = 0$ splits into two curves shifted by a distance of $2\mu_I$. As illustrated in Fig. 5, the structure of the phase diagram in the μ_B - T -plane is structurally altered by an arbitrarily small nonzero isospin chemical potential, even for massive quarks. For a fixed $\mu_I < m_\pi/2$, we find that there are two first order phase transitions at small T when μ_B is increased. Both first order lines end at the same temperature in critical endpoints with a separation proportional to μ_I . The existence of two first order phase transition lines and two critical endpoints might have very important consequences for the numerous phenomenological systems where *both* μ_B and μ_I are nonzero, such as neutron stars or heavy ion collision experiments. Furthermore, it has been shown that relativistic heavy ion collisions experiments might be sensitive to the critical end point in the μ_B - T -plane for $\mu_I = 0$ [54, 55]. Our analysis shows that an increase in μ_I results in a critical end point with a lower value for μ_B , thus making it easier to reach via heavy ion collision experiments. Our analysis also implies that two crossovers separate the quark-gluon plasma and the hadronic phase at small but nonzero baryon and isospin chemical potentials. Therefore the transition between these two phases should appear smoother at $\mu_I \neq 0$ than at $\mu_I = 0$. These results have important phenomenological consequences. It is essential to confirm them by means of lattice QCD simulations or within other models.

Acknowledgments

J. Kogut, K. Splittorff and B. Vanderheyden are acknowledged for useful discussions. K. Splittorff is thanked for a critical reading of the manuscript. D. T. is supported in part by the "Holderbank"-Stiftung. This work was partially supported by the US DOE grant DE-FG-88ER40388 and by the NSF under grant NSF-PHY-0102409.

-
- [1] K. Rajagopal and F. Wilczek, in *At the Frontier of Physics/Handbook of QCD*, edited by M. Shifman (World Scientific, Singapore, 2001), Vol. 3, p. 2061.
- [2] S. Hands, Nucl. Phys. Proc. Suppl. **106**, 142 (2002).
- [3] Z. Fodor and S. D. Katz, JHEP **03**, 014 (2002).
- [4] P. de Forcrand and O. Philipsen, Nucl. Phys. **B642**, 290 (2002).
- [5] C. R. Allton *et al.*, Phys. Rev. D **66**, 074507 (2002).
- [6] M. D'Elia and M. P. Lombardo, arXiv:hep-lat/0209146.
- [7] S. Gupta, arXiv:hep-lat/0202005.
- [8] O. Miyamura, S. Choe, Y. Liu, T. Takaishi, and A. Nakamura, Phys. Rev. D **66**, 077502 (2002).
- [9] R. V. Gavai and S. Gupta, Phys. Rev. D **65**, 094515 (2002).
- [10] A. Barducci, R. Casalbuoni, S. De Curtis, R. Gatto and G. Pettini, Phys. Lett. **B231**, 463 (1989); Phys. Rev. D **41**, 1610 (1990).
- [11] M. A. Halasz, A. D. Jackson, R. E. Shrock, M. A. Stephanov, and J. J. M. Verbaarschot, Phys. Rev. D **58** 096007 (1998).
- [12] J. Berges and K. Rajagopal, Nucl. Phys. **B538**, 215 (1999).
- [13] M. G. Alford, A. Kapustin, and F. Wilczek, Phys. Rev. D **59**, 054502 (1999).
- [14] J. B. Kogut and D. K. Sinclair, Phys. Rev. D **66**, 014508 (2002); Phys. Rev. D **66**, 034505 (2002).
- [15] J. B. Kogut, M. A. Stephanov, and D. Toublan, Phys. Lett. **B464**, 183 (1999).
- [16] J. B. Kogut, M. A. Stephanov, D. Toublan, J. J. M. Verbaarschot, and A. Zhnitsky, Nuc. Phys. **B582**, 477 (2000).
- [17] D. Toublan and J. J. M. Verbaarschot, Int. J. Mod. Phys. B **15**, 1404 (2001).
- [18] D. T. Son and M. A. Stephanov, Phys. Rev. Lett. **86** (2001) 592.
- [19] J. B. Kogut and D. Toublan, Phys. Rev. D **64**, 034007 (2001).
- [20] K. Splittorff, D. T. Son, and M. A. Stephanov, Phys. Rev. D **64**, 016003 (2001).
- [21] T. Schäfer, D. T. Son, M. A. Stephanov, D. Toublan, and J. J. M. Verbaarschot, Phys. Lett. **B522**, 67 (2001).
- [22] F. Sannino and W. Schäfer, Phys. Lett. **B527**, 142 (2002).
- [23] K. Splittorff, D. Toublan, and J. J. M. Verbaarschot, Nucl. Phys. **B620**, 290 (2002).
- [24] K. Splittorff, arXiv:hep-lat/0110226.
- [25] K. Splittorff, D. Toublan, and J. J. M. Verbaarschot, Nucl. Phys. **B639**, 524 (2002).
- [26] G. V. Dunne and S. M. Nishigaki, arXiv:hep-ph/0210219.
- [27] S. Hands, I. Montvay, S. Morrison, M. Oevers, L. Scorzato, and J. Skullerud, Eur. Phys. J. C **17**, 285 (2000).
- [28] R. Aloisio, A. Galante, V. Azcoiti, G. Di Carlo, and A. F. Grillo, arXiv:hep-lat/0007018.
- [29] R. Aloisio, V. Azcoiti, G. Di Carlo, A. Galante, and A. F. Grillo, Phys. Lett. **B493**, 189 (2000).
- [30] Y. Liu, O. Miyamura, A. Nakamura and T. Takaishi, arXiv:hep-lat/0009009.
- [31] S. J. Hands, B. Kogut, S. E. Morrison, and D. K. Sinclair, Nucl. Phys. Proc. Suppl. **94**, 457 (2001).
- [32] R. Aloisio, V. Azcoiti, G. Di Carlo, A. Galante, and A. F. Grillo, Nucl. Phys. **B606**, 322 (2001).
- [33] J. B. Kogut, D. K. Sinclair, S. J. Hands, and S. E. Morrison, Phys. Rev. D **64**, 094505 (2001).
- [34] J. B. Kogut, D. Toublan, and D. K. Sinclair, Phys. Lett. **B514**, 77 (2001); Nucl. Phys. **B642**, 181 (2002).
- [35] D. Bailin and A. Love, Phys. Rept. **107**, 325 (1984).
- [36] D. T. Son, Phys. Rev. D **59**, 094019 (1999).
- [37] M. G. Alford, K. Rajagopal, and F. Wilczek, Phys. Lett. **B422**, 247 (1998).
- [38] R. Rapp, T. Schäfer, E. V. Shuryak, and M. Velkovsky, Phys. Rev. Lett. **81**, 53 (1998).
- [39] E. V. Shuryak and J. J. M. Verbaarschot, Nucl. Phys. **A560**, 306 (1993).
- [40] J. J. M. Verbaarschot, Phys. Rev. Lett. **72**, 2531 (1994).
- [41] J. C. Osborn, D. Toublan, and J. J. M. Verbaarschot, Nucl. Phys. **B540**, 317 (1999).
- [42] P. H. Damgaard, J. C. Osborn, D. Toublan, and J. J. M. Verbaarschot, Nucl. Phys. **B547**, 305 (1999).
- [43] D. Toublan and J. J. M. Verbaarschot, Nucl. Phys. **B603**, 343 (2001).
- [44] D. Toublan and J. J. M. Verbaarschot, Nucl. Phys. **B560**, 259 (1999).
- [45] A. D. Jackson and J. J. M. Verbaarschot, Phys. Rev. D **53**, 7223 (1996).
- [46] M. A. Stephanov, Phys. Rev. Lett. **76**, 4472 (1996).
- [47] M. A. Halasz, J. C. Osborn, M. A. Stephanov, and J. J. M. Verbaarschot, Phys. Rev. D **61**, 076005 (2000).
- [48] J. Ambjorn, K. N. Anagnostopoulos, J. Nishimura, and J. J. M. Verbaarschot, arXiv:hep-lat/0208025.
- [49] B. Vanderheyden and A. D. Jackson, Phys. Rev. D **62**, 094010 (2000).
- [50] B. Vanderheyden and A. D. Jackson, Phys. Rev. D **61**, 076004 (2000).
- [51] B. Vanderheyden and A. D. Jackson, Phys. Rev. D **64**, 074016 (2001).
- [52] S. Pepin and A. Schäfer, Eur. Phys. J. A **10**, 303 (2001).
- [53] B. Vanderheyden and A. D. Jackson, arXiv:hep-ph/0208085.
- [54] M. A. Stephanov, K. Rajagopal, and E. V. Shuryak, Phys. Rev. Lett. **81**, 4816 (1998); Phys. Rev. D **60**, 114028 (1999).
- [55] Y. Hatta and T. Ikeda, arXiv:hep-ph/0210284.
- [56] S. Hands, Nucl. Phys. **A702**, 206 (2002).